6th European Conference on Computational Mechanics (ECCM 6)
7th European Conference on Computational Fluid Dynamics (ECFD 7)
1115 June 2018, Glasgow, UK

INFLUENCE OF CURVED-SHAPE MAGNETS ON THE COOLING PERFORMANCE OF AN AXIAL FLUX PERMANENT MAGNET SYNCHRONOUS MACHINE

Alireza Rasekh[1], Ahmed Hemeida[2], Hendrik Vansompel[2], Peter Sergeant[2,3] and Jan Vierendeels[1]

[1] Department of Flow, Heat and Combustion Mechanics, Faculty of Engineering and Architecture, Ghent University, Ghent, Belgium
E-mail: Alireza.Rasekh@ugent.be, Jan.Vierendeels@ugent.be

[2] Department of Electrical Energy, Systems and Automation, Faculty of Engineering and Architecture, Ghent University, Ghent, Belgium
E-mail: Ahmed.Hemeida@ugent.be, Hendrik.Vansompel@ugent.be, Peter.Sergeant@ugent.be

[3] Flanders Make, The strategic research centre for the manufacturing industry, Belgium

Key words: AFPMSM, CFD, Cooling performance, Curved-shape magnet, Experiment, Windage losses

Abstract. This paper deals with the cooling performance of an axial flux permanent magnet synchronous machine (AFPMSM). The cooling of this machine is mainly achieved by air. The path of the cooling air in an AFPMSM is limited to the small area between the rotor and the stator (air-gap) as well as in the channel being formed between adjacent magnets (air-channel). The rotor disk with the magnets acts as a centrifugal fan resulting in an efficient cooling. Trapezoidal magnets are typically being used in the AFPMSMs. Here, the effects of the curved-shape magnets, instead of conventional trapezoidal magnets, on the convective cooling performance of an AFPMSM are investigated. The case-study is composed of several arbitrary pairs of the rotor disk with their respective curved-shape magnets. CFD simulations are carried out by means of Frozen Rotor (FR) concept to model the cooling airflow in the machine. Besides that, an experiment is conducted to perform this comparative study in order to comprehend the use of curved-shape magnet. The results reveal that the presence of this type of magnets on the rotor would enhance the cooling performance of the AFPMSM. Nevertheless, defining an optimal shape of the curved-shape magnet represents a trade-off problem that should be solved by finding the compromise between the thermal performance and the windage losses.

1 INTRODUCTION

In order to have an efficient design of an AFPMSM, one should minimize the losses in such a device e.g., the electromagnetic losses. Generally, these losses manifest themselves as the production of heat. The operating temperature of an electrical machine can be

controlled by balancing between heat generated and heat removal rate. Controlling the machine operating temperature is crucial, in order to avoid overheating. This means the maximum attainable temperature in the machine is a design constraint that limits the power density [1]. As a consequence, it is imperative to keep the surface temperatures in the allowable range by means of a proper cooling system.

The convective heat transfer in the rotor-stator configuration of an AFPMSM has gained much attention over the past few years [2, 3, 4]. Rasekh et al. [5] demonstrated that the inclusion of the holes in the rotor disk increases the heat transfer removal from the stator, inasmuch as this creates a net radial outflow in the gap region between the rotor and stator. They also introduced correlations for the convective heat transfer in the simplified discoidal system of an AFPMSM [6]. Vansompel et al. [7] has made use of these correlations in a coupled electromagnetic and thermal model of AFPMSM. Their results were successfully validated with the measurement on a 4kW AFPMSM. Very recently, Rasekh et al. [8] developed the correlations for the convective heat transfer coefficients in an AFPMSM taking into account the geometrical parameters of the magnets at the rotor disk. They found out the total heat transfer significantly improves with an increase in the magnet thickness ratio, whereas it decreases as the magnet angle enlarges.

The rotor disk with the magnets on it in an AFPMSM could act as radial air-channels to the circulation of the cooling flow. In order to fully exploit this effect, the influence of the curved-shape magnets instead of the conventional permanent magnet (PM) with trapezoidal shape on the cooling flow characteristics are studied here. Within this context, the literature studies are rather limited. Fawzal et al. [9] performed a comparative study of different fan blade designs of the rotor disk for the cooling of AFPMSM through CFD simulations along with the experimental analysis. It was shown that while the backward-inclined design is appropriate for the windage losses, the radial design results in the better thermal performance with a cost of greater value of windage losses.

The objective of this work is to implement the comparative study to figure out the influence of the curved-shape magnets on the cooling performance of the machine. CFD simulations are performed considering the conjugate heat transfer calculation to model the cooling air characteristic. Additionally, a preliminary experiment is conducted with several arbitrary pairs of the rotor disk with their respective curved-shape magnets.

2 Problem description

Fig. 1 schematically illustrates the rotor-stator configuration in an AFPMSM. The current topology is composed of two rotors, surrounding one stator within a very narrow gap. The geometrical details of the machine are listed in Table 1. There are sixteen magnets on the rotor that are evenly distributed. There exists an annular opening throughout the rotor for the sake of cooling effectiveness. Trapezoidal magnets, forming the radial channels, are typically used in the AFPMSMs. However, curved-shape magnets are being considered here (see Fig. 1).

Fig. 2 gives the geometrical details of one complete curved-shape magnet (front view). The curvature type on the both sides of the magnets is a parabola which is defined by three points: 1) the inner vertex of the magnet (the same as when the trapezoidal magnet

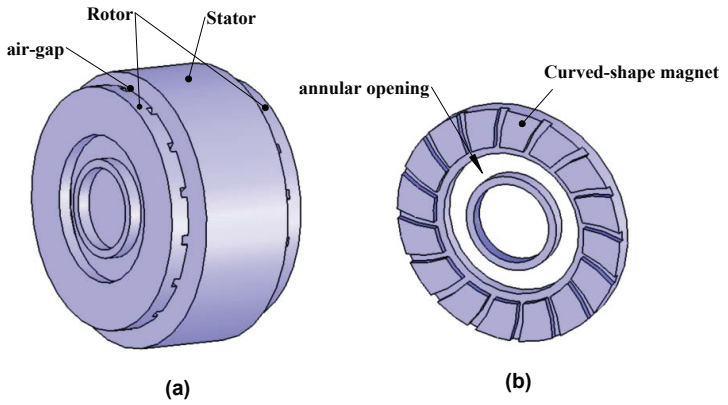

Figure 1: (a) The schematic diagram of an AFPMSM (b) Rotor disk with curved-shape magnets.

Table 1: The geometrical features of the AFPMSM under study.

Parameter	**value (mm)**
Air-gap thickness	1.0
Magnet thickness	4.0
Axial length of Rotor	8.0
Axial length of Stator	60
Radial length of Magnet	24
Shaft diameter	50
Outer radius of Rotor	74
Outer radius of Stator	84
Inner radius of Opening	30
Outer radius of Opening	45

is used), 2) the shoulder of the arc, defined by θ_1, 3) the tip vertex of the magnet, given by θ_2. The magnet angle (α) is kept constant at 18° along the radial direction.

Five cases are being considered in this work including:

- Case 1: trapezoidal magnet ($\theta_1 = \theta_2 = 0°$) with ($\beta_1 = \beta_2 = 0$)
- Case 2: ($\theta_1 = 2°$, $\theta_2 = 6°$) with ($\beta_1 = 100.19°$, $\beta_2 = 110.20°$)
- Case 3: ($\theta_1 = -2°$, $\theta_2 = -6°$) with ($\beta_1 = 79.81°$, $\beta_2 = 69.98°$)
- Case 4: ($\theta_1 = -2.5°$, $\theta_2 = 2.5°$) with ($\beta_1 = 69.10°$, $\beta_2 = 122.67°$)
- Case 5: ($\theta_1 = 2.5°$, $\theta_2 = -2.5°$)with ($\beta_1 = 110.90°$, $\beta_2 = 57.33°$)

The rotation direction in Fig. 2 is counter-clockwise. The corresponding blade angles in turbomachinery are also indicated, where β_1 is the angle made by the magnet at inlet, with the tangent to the inlet radius, and β_2 represents the magnet angle with the tangent at outlet of the air-channel. The graphical illustrations of these rotor disks with their

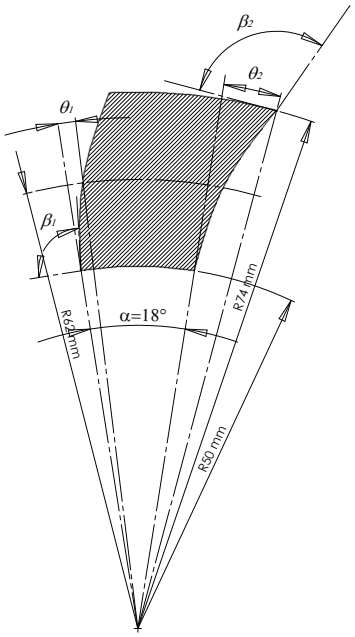

Figure 2: The detailed front-view of the curved-shape magnet ($0 < \theta_1,\ 0 < \theta_2$) (The rotation direction is counter-clockwise.).

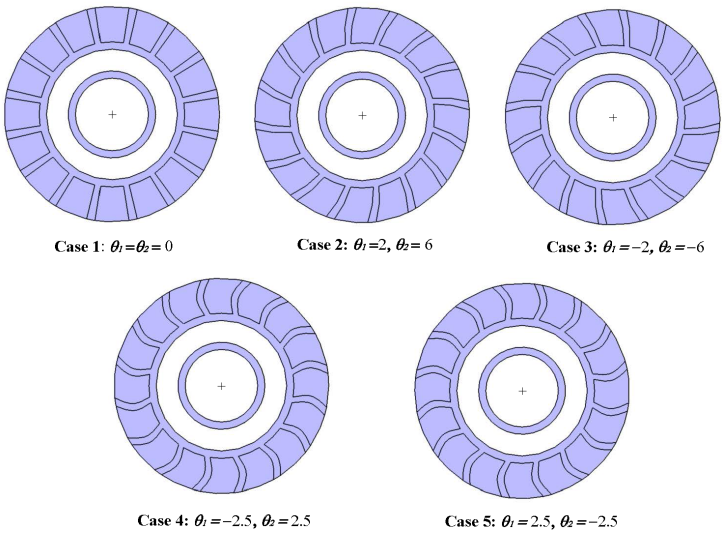

Figure 3: The schematic of the rotor disks with their distinct magnet shapes. (The rotation direction is counter-clockwise.)

distinct shape of the magnets are shown in Fig. 3. In the experiment, for cases 3 & 5, the same disks are used as for the cases 2 & 4, but the rotor is rotated clockwise.

Table 2: The characteristics of the machine used in the test set-up.

Parameter	**Value**	**Unit**
Rated power	4.0	kW
Rated speed	2000	rpm
Rated frequency	333.3	Hz
Rated torque	19	N.m
Number of Magnets	16	-
Number of stator slots	15	-
axial length slot	60	mm
Slot width	12	mm

3 CFD simulations

The 3D CFD simulation are carried out by Ansys FLUENT software to model the cooling air flow in the AFPMSM under investigation. Since the air-channel between the adjacent magnets occupy equal volumes, only one segment of the whole domain is taken into account by making use of the periodic boundary condition. Moreover, half of the stator with one rotor disk is considered using a symmetry plane in the middle of the stator. The computational grid contains more than 3,800,000 cells. The distance of the first node to the solid wall of the rotor is chosen in a way that the value of y^+ is kept below unity. Moreover, a mesh independency study has successfully been performed. The Frozen Rotor (FR) concept, which yields a steady state solution, is applied to model the motion of the rotor. The steady state continuity, momentum and energy equations for the fluid domain will be as follows,

$$\nabla.(\rho_f \overrightarrow{v_r}) = 0 \tag{1}$$

$$\nabla.\left(\rho_f \overrightarrow{v_r} \otimes \overrightarrow{v}\right) + \rho_f(\overrightarrow{\Omega} \times \overrightarrow{v}) = -\nabla p + (\mu + \mu_t)\nabla^2 \overrightarrow{v} \tag{2}$$

$$\nabla.\left(\rho_f \overrightarrow{v_r} h_f + p(\overrightarrow{\Omega} \times \overrightarrow{r})\right) = \nabla.\left((k_f + k_t)\nabla T\right) \tag{3}$$

In the above, $\overrightarrow{v_r}$ is the relative velocity with respect to the rotating frame, $\overrightarrow{v}$ is the absolute velocity in the stationary frame, $\overrightarrow{\Omega}$ represents the rotational velocity vector of the rotating domain, ρ_f indicates the air density, h_f is the specific enthalpy of air, μ is molecular viscosity and μ_t is the turbulent viscosity, k_f is air thermal conductivity and k_t denotes the turbulent thermal conductivity. The turbulent properties are computed from the $k-\omega$ SST turbulence model.

The losses in the machine are introduced as volumetric heat sources in the solid parts. Conjugate heat transfer (CHT) calculations are performed, as the flow and heat transfer of the cooling air should be solved at the same time with the energy equation in the solid domain. As a matter of fact, the governing equations in each of the fluid and the solid regions are solved iteratively. The fluid/solid interfaces are employed to couple the energy equations between the fluid and solid domain to ensure the continuity of temperature and the conservation of energy. Inside the solid region, the energy equation is written as,

$$\nabla.\left(k_s \nabla T\right) + S_h = 0 \tag{4}$$

where S_h represents the volumetric heat source, and k_s is thermal conductivity of the solid parts. It is assumed that the thermal conductivities of the machine parts comprising the rotor, the magnet and the stator are uniform, isotropic and constant with temperature.

4 Experimental Set-up

An AFPMSM prototype, shown in Fig. 4, is manufactured to evaluate the thermal performance of the machine. The main characteristics of this test set-up are listed in Table 2. This prototype is used as a generator. It is powered by an induction machine, and the rotational speed is controlled by an industrial inverter. Note that the rotor disks with their dummy magnets (shown in Fig. 5) have the same geometrical features as in the CFD modeling.

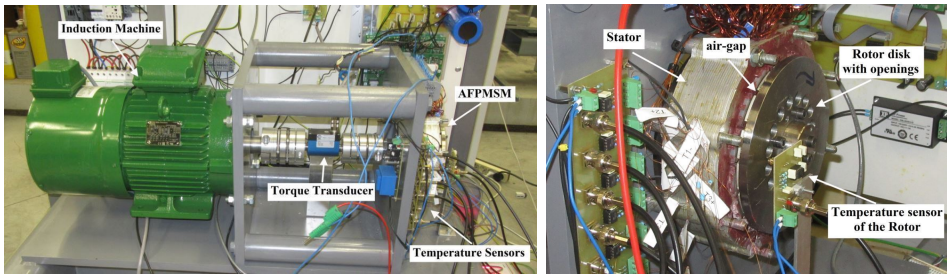

(a) (b)

Figure 4: (a) Experimental set-up (b) close-up of the prototype.

The body of the rotor disk is also made of aluminium. On the stator side, the heat is generated by Joule losses. At full load of the machine, about 100 W power loss is present in the entire stator. The experiments are conducted at rotational speeds of 1000 and 2000 rpm. Temperature sensors are inserted in the test set-up to measure the temperature at different parts of the machine. An infrared temperature sensor ZTP-135SR is used to measure the rotor temperature. To record the stator winding temperature, a PT100 platinum resistance thermometer is placed inside it. The room temperature of the laboratory where the measurement carried out is around 25°C. In order to ensure that the machine has reached the thermal steady state condition, the temperatures are monitored with time. Typically, a steady state temperature was reached after 2.5 hours of running time.

5 Results and discussion

In this section, the effects of using curved-shape magnets on the thermal efficiency and the windage losses are elaborately explained.

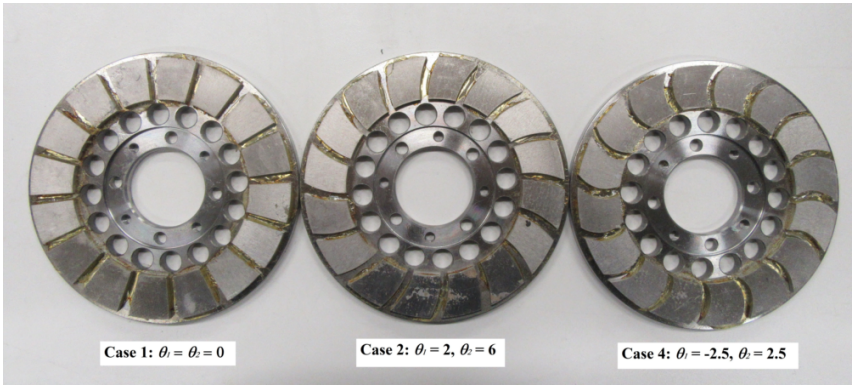

Figure 5: The rotor disks with dummy magnets used in the experiment.

5.1 CFD simulation results

5.1.1 Cooling air characteristics

Due to the compact structure of AFPMSMs, the appropriate thermal modeling is one of the main design issues. A good way of improving the efficiency of the cooling system is to induce flow from the surrounding cooler air into the machine, in particular to the air-channel. Therefore, we focus on the flow characteristics inside this region.

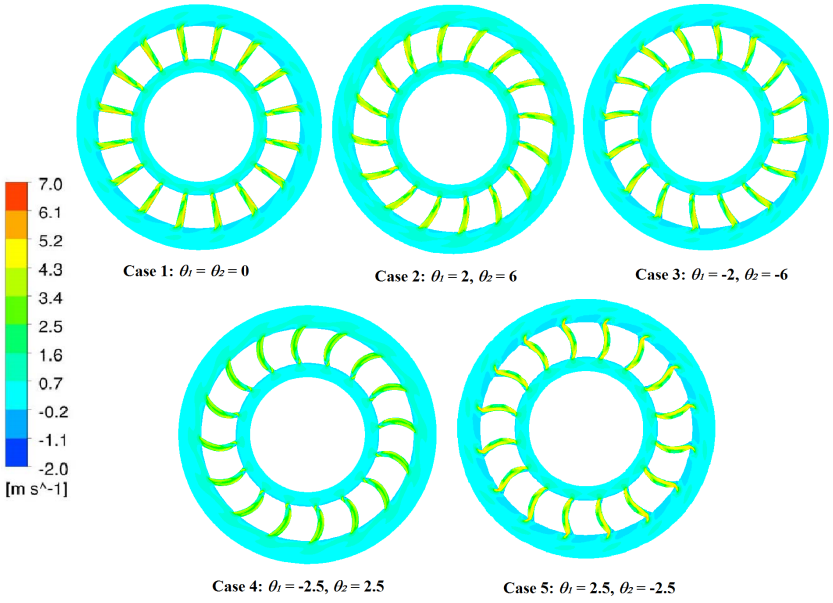

Figure 6: Radial velocity contours in the air-channel for various curved-shape magnets at $\omega = 1000$ rpm. (The rotation direction is counter-clockwise.)

Fig. 6 elucidates the contour of the radial velocity in the air-channel for several curved-shape magnets at rotational speed of 1000 rpm when the direction of the rotation is counter-clockwise. It is observed that the use of the rotor disk case 5 ($\theta_1 = 2.5, \theta_2 = -2.5$)

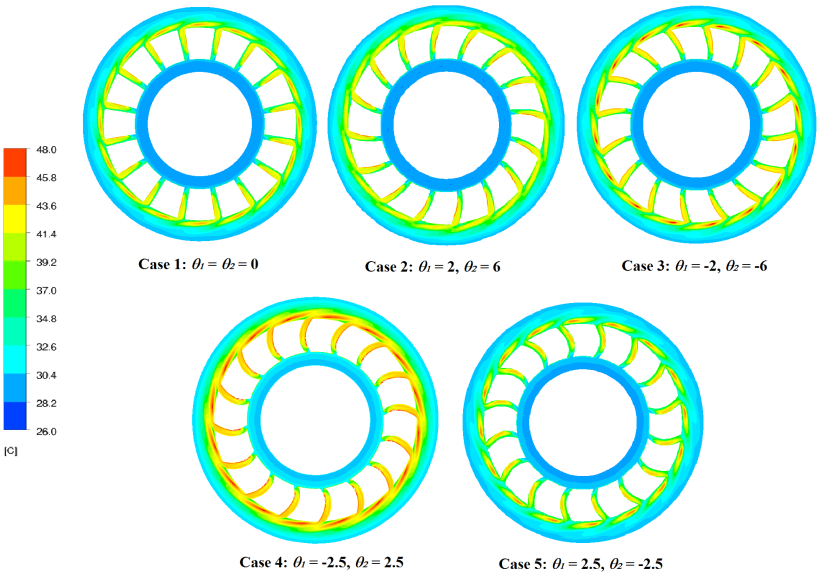

Figure 7: Temperature contours in the air-channel for various curved-shape magnets at $\omega = 1000$ rpm. (The rotation direction is counter-clockwise.)

results in the strongest radial outflow at the periphery of the air-channel, whereas the application of the case 4 ($\theta_1 = -2.5, \theta_2 = 2.5$) leads to the weakest airflow directed in the space between the magnets.

To gain more detailed insight about the flow field, Table 3 provides the data for the incoming mass flow rate of the cooling air to the machine passing through the annular opening with different curved-shape magnets. It is found that the case 5 ($\theta_1 = 2.5, \theta_2 = -2.5$) gives rise to the highest mass flow rate of the cooling air for both rotational speeds of 1000 and 2000 rpm. These findings support the results observed in the radial velocity contour alongside the air-channel. From this Table, it is also seen that the trapezoidal magnets are the second best. Therefore, it can be concluded that having the curved-shape magnet does not necessarily enhance the amount of the cooling air entering to the AFPMSM as compared to the trapezoidal magnets, and it is the shape of the curvature that plays the essential role.

Table 3: Mass flow rate (kg/s) passing through the annular opening for various curved-shape magnets and rotational speeds.

	different curved-shape magnets				
Rotational speed (rpm)	($\theta_1 = \theta_2 = 0$)	($\theta_1 = 2$, $\theta_2 = 6$)	($\theta_1 = -2$, $\theta_2 = -6$)	($\theta_1 = -2.5$, $\theta_2 = 2.5$)	($\theta_1 = 2.5$, $\theta_2 = -2.5$)
1000	0.00116	0.00111	0.00102	0.00095	0.00118
2000	0.00282	0.00265	0.00250	0.00223	0.00297

Besides the effects of the curved-magnet on the flow structure, the trends for the air temperature distribution are equally important. Fig. 7 illustrates the temperature contours in the air-channel between the magnets when each of the five disks is utilized.

The use of the curved-shape magnets with ($\theta_1 = 2.5, \theta_2 = -2.5$) leads to coldest air in this region as compared to other rotor disks examined here. By contrast, the curved-shape magnet with ($\theta_1 = -2.5, \theta_2 = 2.5$) brings about the highest air temperature in the air-channel. The lower air temperature represents the effectiveness of the corresponding rotor disk in the heat losses evacuation.

5.1.2 Windage losses

Another issue that can be affected by the shape of the magnets is the windage power loss. The total windage losses are evaluated by accumulating the power associated with the aerodynamic forces (viscous or pressure) against rotary parts of the machine.

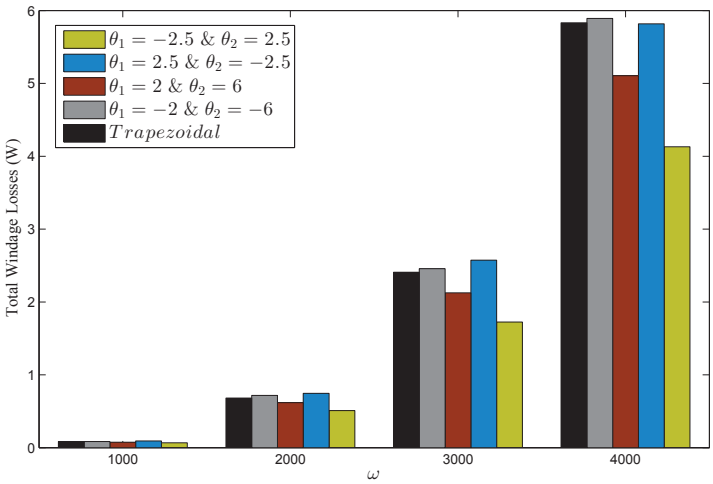

Figure 8: The overall windage losses in the AFPMSM for various curved-shape magnets at different rotational speeds.

Fig. 8 discloses the effect of the curved-shape magnets on the overall windage losses in the machine at different rotational speeds, based on the results of the CFD simulations. The lowest values of the windage losses can be achieved by using the curved-shape magnet with ($\theta_1 = -2.5, \theta_2 = 2.5$). This trend is very noticeable at the higher rotational speed, e.g., at 4000 rpm. Furthermore, the forward curved rotors (Case 3 & Case 5) result in greater windage power losses as compared to the backward curved rotors (Case 2 & Case 4), which is quite expected from the turbomachinery point of view. This tendency could be attributed to the stronger radial flow by using forward curved rotor disk, shown in Fig. 6.

5.2 Experimental results

The measured values of the steady state temperatures of the rotor disk and the stator are used to evaluate the effectiveness of the curved-shape magnets in the full load of the prototype.

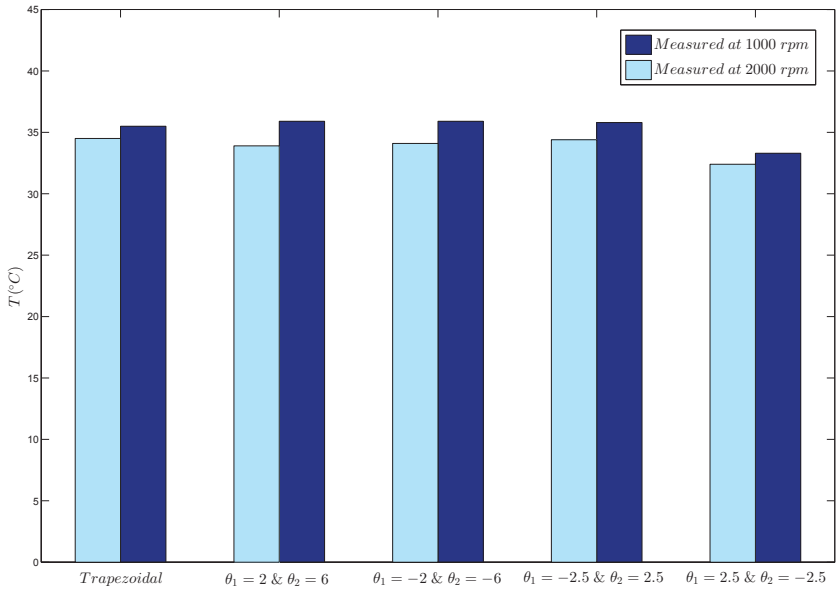

(a) Rotor temperature

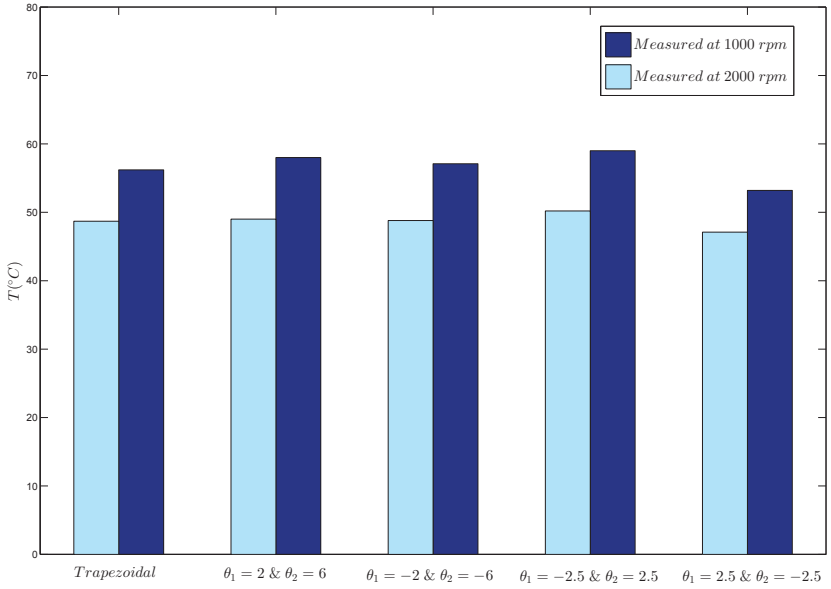

(b) Stator temperature

Figure 9: Comparison between the results of CFD simulations and the experimental data according to various curved-shape magnets (a) rotor temperature (b) stator temperature.

Fig. 9 demonstrates the temperatures of the rotor and the stator from the measurement data at the rotational speeds of 1000 and 2000 rpm. It is found that the use of the rotor disk with the curved-shape magnet of $(\theta_1 = 2.5, \theta_2 = -2.5)$ leads to the lowest temperature of the rotor, i.e., about 33.3°C at 1000 rpm, even though the temperature reduction is not very remarkable. In fact, the difference between the maximum tempera-

ture of the rotor disk with ($\theta_1 = 2.5, \theta_2 = -2.5$) and the minimum temperature achieved by the curved-shape magnet of ($\theta_1 = -2.5, \theta_2 = 2.5$) is less than 3°C according to the measured data at the rotational speed of 1000 rpm. This difference becomes even smaller once the rotational speed reaches 2000 rpm.

Similar to the results for the temperature of the rotor disk, it is observed that the use of the curved-shape magnet ($\theta_1 = 2.5, \theta_2 = -2.5$) brings about the lowest stator winding temperature (about 47°C at 2000 rpm) as compared to other magnets examined in this work. The experimental results also show that an increase in the rotational speed from 1000 to 2000 rpm results in the stator winding temperature drops from 56°C to about 48°C when the trapezoidal magnets ($\theta_1 = \theta_2 = 0$) are used.

6 CONCLUSIONS

This paper dealt with the effect of the curved-shape magnets at the rotor disk on the cooling performance and windage losses in an AFPMSM. Five pairs of rotor disks with their distinct dummy magnets were considered as the case-study. CFD simulation were implemented to model the cooling air flow in the channel between magnets and the small gap between rotor and stator. Moreover, the numerical findings were used to assess the windage power losses. An experimental analysis was also undertaken by manufacturing the same rotor disks with the curved-shape magnets as in the numerical thermal modeling.

The CFD results revealed that the strongest radial outflow at the periphery of the air-channel with the coldest air in this region is achieved for the curved-shape magnet of ($\theta_1 = 2.5, \theta_2 = -2.5$). Moreover, it was shown that to attain the lowest windage losses the curved-shape magnet with ($\theta_1 = -2.5, \theta_2 = 2.5$) could be the best choice among the other magnets tested here. From the CFD results, an increase in rotational speed of the rotor from 1000 to 4000 rpm results in the windage losses increase from 0.08 to 5.8W.

The steady state temperature of the rotor and stator were measured for the various curved-shape magnets at different rotational speeds. The measurement data indicated that there is about 8°C temperature reduction in the stator winding for the trapezoidal magnets when the rotational speed goes up from 1000 to 2000 rpm. Furthermore, it was demonstrated that the use of the rotor disk with the curved-shape magnets ($\theta_1 = 2.5, \theta_2 = -2.5$) results in the lowest temperature on the rotor and stator. However, the temperature differences between the best choice of the rotor disk with the worst one is not very remarkable, e.g., only about 3°C in the stator temperature at 2000 rpm.

In summary, defining an optimal shape of the curved-shape magnet at the rotor disk represents a trade-off problem that should be solved by finding the compromise between the thermal performance and the windage losses. For the application presented here, use of the curve-shape magnet with ($\theta_1 = 2.5, \theta_2 = -2.5$) is recommended for the cooling purposes, whereas the choice of ($\theta_1 = -2.5, \theta_2 = 2.5$) is advantageous in the windage power losses point of view.

REFERENCES

[1] Chapman, S. *Electrical machinery fundamentals.* New York: McGraw Hill, 4th Edition, 2005.

[2] Hong, C. *Thermal Modelling of the Ventilation and Cooling Inside Axial Flux Permanent Magnet Generator.* (Doctoral thesis), School of Engineering and Computer Science, Durham University, UK, 2011.

[3] Wrobel, R. Vainel, G. Copeland, C. Duda, T. Staton, D. Mellor, P. Investigation of mechanical loss and heat transfer in an axial-flux PM machine. *IEEE Energy Conversion Congress and Exposition (ECCE)* (2013) 4372-4379.

[4] Pyrhönen, J. Lindh, P. Polikarpova, M. Kurvinen, E. Naumanen, V. Heat-transfer improvements in an axial-flux permanent-magnet synchronous machine. *Appl. Therm. Eng* (2015) 245-251.

[5] Rasekh, A. Sergeant, P. Vierendeels, J. A parametric-CFD study for heat transfer and fluid flow in a rotor-stator system. *11th World Congress on Computational Mechanics; 5th European Conference on Computational Mechanics; 6th European Conference on Computational Fluid Dynamics* (2014) vol. iiiv, 4475-4483.

[6] Rasekh, A. Sergeant, P. Vierendeels, J. Convective heat transfer prediction in disk-type electrical machines. *Appl. Therm. Eng* (2015) 245-251. 91. 778-790.

[7] Vansompel, H. Rasekh, A. Hemeida, A. Vierendeels, J. Sergeant, P. Coupled electromagnetic and thermal analysis of an axial flux PM machine. *IEEE Trans. Magn* (2015) 51 (11) 1-4.

[8] Rasekh, A. Sergeant, P. Vierendeels, J. Fully predictive heat transfer coefficient modeling of an axial flux permanent magnet synchronous machine with geometrical parameters of the magnets. *Appl. Therm. Eng* (2017) (110) 1343-1357.

[9] Fawzal, A.S. Cirstea, R.M. Gyftakis, K. Woolmer, T.J. Dickison, M. Blundell, M.V. The fan design impact on the rotor cooling of axial flux permanent magnet machines. *International Conference on Electrical Machines (ICEM)* (2016) 2727-2733.